Protein Tyrosine Phosphatase φ Regulates Paxillin Tyrosine Phosphorylation and Mediates Colony-Stimulating Factor 1-Induced Morphological Changes in Macrophages

FIONA J. PIXLEY,[1] PIERRE S. W. LEE,[1] JOHN S. CONDEELIS,[2] AND E. RICHARD STANLEY[1]*

Department of Developmental and Molecular Biology[1] and Department of Anatomy and Structural Biology and the Analytical Imaging Facility,[2] Albert Einstein College of Medicine, Bronx, New York 10461

Removal of colony-stimulating factor 1 (CSF-1) causes macrophages to round up and to increase their expression of protein tyrosine phosphatase φ (PTPφ). This is accompanied by the disruption of focal complexes and the formation of ruffles. Here we have overexpressed wild-type (WT) PTPφ and a phosphatase-inactive (C325S) mutant in a macrophage cell line in the presence and absence of CSF-1. In the presence of CSF-1, WT PTPφ induces cell rounding and ruffle formation, while C325S PTPφ has no effect. In contrast, in CSF-1-starved cells, C325S PTPφ behaves in a dominant negative fashion, preventing rounding and ruffling. Furthermore, C325S PTPφ increases adhesion in cycling cells, while WT PTPφ enhances motility. In WT PTPφ-overexpressing cells, the focal contact protein paxillin is selectively depleted from focal complexes and specifically dephosphorylated on tyrosine. In contrast, paxillin is hyperphosphorylated in C325S PTPφ-expressing cells. Moreover, a complex containing PTPφ, paxillin, and a paxillin-associated tyrosine kinase, Pyk2, can be immunoprecipitated from macrophage lysates, and the catalytic domain of PTPφ selectively binds paxillin and Pyk2 in vitro. Although PTPφ and Pyk2 do not colocalize with paxillin in focal complexes, all three proteins are colocalized in dorsal ruffles. The results suggest that paxillin is dephosphorylated by PTPφ in dorsal ruffles, using Pyk2 as a bridging molecule, resulting in a reduced pool of tyrosine-phosphorylated paxillin available for incorporation into focal complexes, thereby mediating CSF-1 regulation of macrophage morphology, adhesion, and motility.

Macrophages are terminally differentiated cells of the mononuclear phagocyte lineage and are specialized for locomotion and phagocytosis. Colony-stimulating factor 1 (CSF-1) is the primary regulator of the survival, proliferation, and differentiation of mononuclear phagocytic cells (12, 39) as well as macrophage morphology and motility (9, 45). Cells of the BAC1.2F5 mouse macrophage cell line have retained many characteristics of primary macrophages, including dependence on CSF-1 for survival and proliferation (30) and a pleiomorphic but adherent phenotype. When starved of CSF-1, BAC1.2F5 cells round up, retract their pseudopodia (9), and eventually die. With the addition of CSF-1 to quiescent cells, the CSF-1 receptor (CSF-1R [c-*fms*]) is rapidly activated, leading to receptor autophosphorylation and tyrosine phosphorylation of a number of cytoskeletal proteins and cytoplasmic proteins associated with signaling (26, 47). Morphological changes are also effected rapidly upon CSF-1 stimulation, with macrophage spreading and extension of lamellipodia and formation of ruffles on the cell surface (9), followed by cell polarization and increased motility (3, 45).

Tyrosine phosphorylation is a critical control mechanism for the regulation of cell survival, proliferation, morphology, and motility. The balance of cellular tyrosine phosphorylation is controlled by the coordinated actions of protein tyrosine kinases and protein tyrosine phosphatases (PTPs). A number of PTPs have been implicated in receptor tyrosine kinase (RTK)

signaling and proliferative pathways, in particular the cytosolic, SH2 domain-containing PTPs SHP-1 and SHP-2 (42). Cell morphology and motility are regulated both by RTK-linked intracellular signaling pathways and by interactions between the cell and its extracellular matrix (ECM) (29). ECM ligand-mediated activation of integrin cell adhesion receptors (24) triggers tyrosine phosphorylation in a variety of cell lines (15), including the tyrosine phosphorylation of focal adhesion kinase (FAK), Pyk2, paxillin, and p130^{cas} (6, 11, 17, 32). These phosphorylated proteins are concentrated at points of interaction between the ECM and the cytoskeleton, known as focal contacts. Paxillin is one of the more highly tyrosine phosphorylated focal adhesion proteins and requires the coordinated actions of both the FAK/Pyk2 and the Src family kinases to be fully tyrosine phosphorylated (36).

As in more rigid cells such as fibroblasts, the dynamic shape and motility of macrophages is controlled by cell-ECM interactions. However, their focal contacts are much smaller and are termed focal complexes (2). Tyrosine kinases implicated in the phosphorylation of focal adhesion proteins and in focal adhesion formation include FAK, Pyk2, and the Src family kinases (15). Fewer PTPs are known to dephosphorylate focal adhesion proteins, although two cytoplasmic PTPs, PTP-PEST and PTP1B, have been shown to specifically dephosphorylate p130^{cas} (16, 19, 27). The cytoplasmic enzymes PTP-PEST, PTP1B, and SHP-2 and the tumor suppressor PTEN appear to play important roles in fibroblast focal contact formation, spreading, and migration (4, 5, 20, 21, 27, 48), while SHP-1 deficiency results in an increase in macrophage spreading (34). Several other PTPs have been shown to be localized to focal contacts or important in cell adhesion. LAR is a membrane-

spanning PTP with fibronectin type III (FNIII) repeats in its extracellular domain (ECD) (40). It is localized to focal contacts in a distribution that suggests it may be important in their disassembly (38). FNIII repeats may be involved in cell adhesion (37, 43). The PTPμ family of PTPs, which contain FNIII repeats in their ECDs, interact homophilically to mediate cell-cell aggregation (10, 14, 35). Several *Drosophila* PTPs with FNIII repeats in their ECDs and a mammalian PTP, PTPζ/RPTPβ, have been implicated in neuronal adhesion and motor axon guidance (42).

PTPφ is a complex PTP with at least five different isoforms (33, 41). The largest isoforms each contain an identical large ECD with eight FNIII repeats and are expressed in brain and kidney. The remaining isoforms of PTPφ, which are selectively expressed in macrophages (33) and B cells (1), comprise two membrane-spanning molecules with an identical, very short ECD lacking FNIII repeats and a cytosolic enzyme. Thus, PTPφ could be involved in cell-cell adhesion of stationary cells in the brain and kidney yet may mediate different functions, such as motility and/or phagocytosis, in macrophages. In the present study, we have analyzed BAC1.2F5 macrophages overexpressing either the wild-type (WT) or a phosphatase-inactive (C325S) form of the larger membrane-spanning isoform of PTPφ in order to understand its function.

MATERIALS AND METHODS

Cells. BAC1.2F5 macrophages (30) and subclones were maintained in supplemented α-modified minimal essential medium (α+MEM) (Life Technologies, Gaithersburg, Md.) containing 10% newborn calf serum and 36 ng of recombinant human CSF-1 (a gift from Chiron, Palo Alto, Calif.) per ml as previously described (30). BAC1.2F5 cells were subcloned, and one subclone, BAC1.2F5.2, with properties similar to the parental clone, was used for all studies except where otherwise indicated. The PE501 retrovirus packaging fibroblast cell line was grown in α+MEM containing penicillin and streptomycin (100 mg of each/liter) and supplemented with 10% fetal calf serum (Life Technologies).

Cellular expression of PTPφ protein. Cells were washed in phosphate-buffered saline (PBS), lysed in NP-40 lysis buffer (10 mM Trizma base, 50mM NaCl, 30 mM sodium pyrophosphate, 50mM NaF [pH 7.0] containing 5 μM ZnCl₂, 0.5 mM sodium orthovanadate, 0.5% NP-40, 1 mM benzamidine plus 10 μg of leupeptin and 10 μg of aprotinin per ml) at 4°C, then vortexed and centrifuged at 13,000 × *g* for 30 min. Western blotting was performed as previously described (33) using a rabbit anti-PTPφ antiserum raised to a full-length glutathione-*S*-transferase (GST)-PTPφ fusion protein with the modification that NP-40-soluble lysates were used for Western blots because the resulting PTPφ bands were sharper and more distinct. When NP-40-insoluble pellets were solubilized in sodium dodecyl sulfate (SDS) sample buffer, and the pellets and lysates were compared by SDS-polyacrylamide gel electrophoresis (PAGE) analysis and PTPφ Western blotting, >95% of cellular PTPφ partitioned to the NP-40-soluble fraction (data not shown).

Site-directed mutagenesis and pLXSN constructs. Although the 43-kDa isoform of PTPφ is more highly expressed than the 47-kDa variant, the difference between their levels of expression in macrophages can vary considerably (compare Fig. 2A with 2C) and it is not apparent how they differ functionally. Their expression patterns are coordinately regulated with respect to CSF-1-induced and density-induced changes and to their subcellular localization (data not shown), and in human B cells, the 47-kDa isoform is more highly expressed than the 43-kDa isoform (1). The 47-kDa isoform was selected for retroviral expression in BAC1.2F5.2 cells. Using double-stranded oligonucleotides encoding the 9-amino-acid hemagglutinin (HA) tag, an HA tag was inserted in frame into the carboxyl-terminal end of PTPφ. The Transformer site-directed mutagenesis kit (Clontech, Palo Alto, Calif.) was then used according to the manufacturer's protocol to mutate the essential cysteine (C325) of PTPφ to serine. The resulting HA-tagged WT PTPφ and C325S PTPφ constructs were ligated into the *Eco*RI site of the pLXSN retroviral expression vector (28), and the final constructs were checked by sequencing.

Transfection, retroviral infection, and stable cell line selection. PE501 fibroblasts were transfected with either the pLXSN vector, WT PTPφ, or C325S

PTPφ using Lipofectamine (Life Technologies) and retrovirus-conditioned medium prepared from confluent cultures as previously described (28). BAC1.2F5 cells were seeded onto 60-mm tissue culture dishes (2 × 10⁵ cells/dish, 4 ml of medium/dish) with Polybrene (5 μg/μl). The following day, the medium was removed, 0.5 ml of the undiluted retrovirus-conditioned medium was added, and the plates were incubated at 37°C with shaking every 15 min for 90 min. Medium (4 ml) was then added to the cells overnight, and the medium was changed the next day. Two days after infection, the cells were passaged 1:10 into 0.5-mg/ml G418, and single-cell isolates of G418-resistant colonies were used to establish 20 stable cell lines per construct.

Analysis of cell growth. Cells were seeded in 35-mm tissue culture plates at 1 × 10⁴ to 2 × 10⁴ cells/plate in 2 ml of medium. Cell counts were performed in triplicate from the second day after plating. For determination of proliferation rates, fresh medium containing CSF-1 (36 ng/ml) was added every 2 days for 6 days and then daily for the remainder of the experiment. For determination of survival rates, growth medium was replaced by CSF-1-free medium on day 1 and replenished every 2 days.

Phase-contrast light microscopy and scanning EM. Cells were plated on 13-mm circular glass coverslips in 35-mm dishes and grown to 70% confluence. The coverslips were rinsed with serum-free medium, and in order to prevent agonal membrane artifacts, common with slower fixatives, the cells were fixed quickly with 2 ml of 1% osmium tetroxide in 0.1 M cacodylate for 5 s at room temperature. This was followed by two consecutive 60-min fixations with 2.5% glutaraldehyde in 0.1 M cacodylate at room temperature and a final wash in 0.1 M cacodylate for 10 min. The fixed cells were then dehydrated through a graded series of ethanol, critical point dried using liquid carbon dioxide in a Tousimis Samdri 790 critical point drier (Rockville, Md.), sputter coated with gold-palladium in a Denton Vacuum Desk-1 sputter coater (Cherry Hill, N.J.), mounted, and viewed in a JEOL JSM6400 scanning electron microscope (Peabody, Mass.) using an accelerating voltage of 5 kV for electron microscopy (EM).

Immunofluorescence staining. Cells were seeded onto 22-mm-square fibronectin-coated glass coverslips (Becton Dickinson, Bedford, Mass.) in six-well tissue culture plates. When 70 to 80% confluent, cells were rinsed with 1X PBS at 37°C, fixed in 3.7% formaldehyde in buffer F (5 mM KCl, 137 mM NaCl, 4 mM NaHCO₃, 4 mM KH₂PO₄, 1.1 mM Na₂HPO₄, 2 mM MgCl₂, 5 mM PIPES [piperazine-*N*,*N'*-bis(2-ethanesulfonic acid), pH 7.2], 2 mM EGTA, 5.5 mM glucose) for 5 min at 37°C, extracted in 0.5% Triton X-100 in buffer F for 20 min at room temperature, and washed in 0.1 M glycine in buffer F for 10 min at room temperature. The coverslips were washed five times for 5 min in 1X Tris-buffered saline (TBS) and blocked with 1% bovine serum albumin (BSA)–10% goat serum in 1X TBS for 20 to 30 min (with tetramethyl rhodamine isocyanate [TRITC]-phalloidin at 0.5 μM [Molecular Probes, Eugene, Oreg.] if staining for F-actin filaments). The cells were incubated at room temperature for 45 to 60 min with primary antibody, then washed three times for 10 min in 1% BSA in 1X TBS, and incubated with secondary antibody for 45 to 60 min at room temperature before a final series of three 10-min washes in 1% BSA in 1X TBS. If two primary antibodies were used, the antibodies were added sequentially, and each addition was directly followed by incubation with the respective secondary antibodies. The coverslips were mounted in Slow Fade (Molecular Probes), and all samples were examined under an Olympus 1X70 inverted microscope with images recorded using a Photometrics CH1 cooled charge coupled device (CCD) camera. Antibodies used included an affinity-purified rabbit anti-PTPφ antibody directed to a C-terminal peptide (CISDVIYENVSKS); a polyclonal antiphosphotyrosine antibody (P11230; Transduction Labs, Lexington, Ky.), anti-Golgi (TGN38, Affinity Bioreagents, Golden, Colo.), anti-β1-integrin (9EG7; gift of Dietmar Westweber), and anti-α4-integrin (PS/2; gift of Sue Craig) rat monoclonal antibodies (MAbs); and antiphosphotyrosine (anti-PTyr; PT66; Sigma), antipaxillin (P13520; Transduction Labs), antivinculin (Sigma), and anti-β-tubulin (XIV17.16; gift of Anne Johnson) mouse MAbs. Quantitation of focal complex tyrosine phosphorylation was carried out by measuring mean pixel intensities using IPLab Spectrum software (Scanalytics, Fairfax, Va.). A grid of concentric circles (0.6-mm radial increments) was centered on the nuclear region of TRITC-phalloidin labeled cells for morphometric quantitation of F-actin bundle numbers. Every bundle-grid intersection was counted for each cell, and 25 cells were analyzed to determine the mean F-actin bundle count per cell for each cell line.

Adhesion assay. Using fibronectin- or laminin-coated 24-well plates (Becton Dickinson), 5 × 10⁴ cells were plated per well, in triplicate, and allowed to adhere at 37°C for various periods of time. The cells were then gently rinsed twice with warmed PBS and fixed for 7 min at 37°C in 3.7% formaldehyde, and adherent cells were counted.

Wound-healing assay. Cells were plated onto tissue culture dishes and grown to confluence before scoring with a sterile 200-μl micropipette tip. Normal

medium was changed daily, and the wounds were photographed at intervals until they were occluded by incoming cells.

Immunoprecipitation. Subconfluent cultures of cells in 100-mm dishes were treated with CSF-1 with or without pervanadate where indicated, rinsed in ice-cold PBS, scraped into 200 μl of lysis buffer at 4°C, vortexed, and centrifuged at 13,000 × g for 30 min. The supernatant was incubated overnight with 5 μg of antibody and 40 μl of protein A-Sepharose 4B beads (Zymed, San Francisco, Calif.) at 4°C and then centrifuged at 13,000 × g at 4°C for 30 s. The beads were washed five times in wash buffer (lysis buffer without leupeptin and aprotinin) at 4°C and once in double distilled water, and the proteins were eluted with half the bead volume of 3X SDS sample buffer. Eluted proteins were resolved by SDS–10% PAGE and Western blotted as previously described (33). The antibodies used were anti-PTyr antibody RC20H (Transduction Laboratories), anti-C-terminal PTPφ (for immunoprecipitation), anti-GST-PTPφ antiserum (for Western blotting), antipaxillin (Transduction Laboratories) and anti-Pyk2 (Transduction Laboratories) MAbs, and polyclonal goat anti-CSF-1R antibody (26).

In vitro binding assay. C325S-PTPφ-expressing BAC1.2F5 cells were incubated with CSF-1 for 10 min at 37°C and then with pervanadate for a further 10 min in order to increase the number and intensity of phosphotyrosyl proteins, as described (26). The catalytic domains of WT PTPφ and C325S PTPφ (from 130QFEELKLIG to VQLMWLRKK389) were subcloned into the pGEX-KG vector, and the GST-PTPφ fusion proteins were expressed and affinity purified with glutathione-Sepharose beads (Pharmacia Biotech, Piscataway, N.J.) (22). The NP-40-soluble BAC1.2F5 cell lysates were cleared three times with GST bound to glutathione-Sepharose beads for 2 h each at 4°C. The supernatants were incubated overnight at 4°C with GST or GST-PTPφ fusion proteins bound to glutathione-Sepharose beads. The beads were washed five times in wash buffer with 0.5% NP-40 and twice in wash buffer with 0.8% octylglucoside before elution with half the bead volume of 3X SDS sample buffer at 65°C for 15 min. Eluted proteins were resolved by 10% acrylamide SDS-PAGE and Western blotted as above.

Far Western analysis. Cells were upregulated for 24 h and then stimulated with CSF-1 for 15 min before immunoprecipitation was carried out as described above, using an anti-PTyr antibody (PY20; Transduction labs). Bound proteins were eluted with 15 mM phenylphosphate, resolved by SDS–10% PAGE, and Western blotted as described for phosphotyrosyl proteins. The membrane was stripped and probed with a GST-PTPφ catalytic domain fusion protein (2.5 μg/ml) under conditions in which the SHP-1 SH2 domains were shown to bind the physiological substrate PIR-B (for paired immunoglobulin (Ig)-like receptor B) (8).

RESULTS

PTPφ is expressed in the Golgi apparatus and in dorsal ruffles of macrophages and its expression increases with removal of CSF-1. Immunofluorescent staining was carried out to determine the subcellular localization of PTPφ. Bright staining of PTPφ in the Golgi apparatus was easily visible using confocal microscopy and the Golgi marker TGN38 for colocalization (Fig. 1a to e). However, more sensitive cooled CCD imaging was necessary to demonstrate the punctate distribution of PTPφ staining on the plasma membrane (Fig. 1d and e) PTPφ was also clearly seen in membrane ruffles when the plane of focus was raised (Fig. 1f).

The antibody chosen to examine the subcellular distribution of PTPφ was a C-terminal antipeptide antibody that recognizes the 47-, 43-, and 33-kDa isoforms. However, the 33-kDa isoform is expressed at such low levels that we have not been able to demonstrate its protein product by Western blotting (33). The two membrane-spanning isoforms found in macrophages differ by a short, hydrophobic juxtamembrane domain. It has not been possible to produce antibodies that discriminate between them. A second antipeptide antibody directed to a short sequence of PTPφ immediately upstream of the catalytic domain showed less intense but similar staining of PTPφ in the Golgi apparatus and plasma membrane (data not shown).

PTPφ mRNA expression in BAC1.2F5 cells has been shown previously to be regulated by CSF-1 (33). Removal of CSF-1 resulted in a threefold increase in the expression of the membrane-spanning 43- and 47-kDa isoforms of PTPφ in BAC1.2F5 cells (Fig. 2A), and within 8 h of restimulation of quiescent cells with CSF-1, PTPφ expression had decreased to levels approximating those seen in asynchronously cycling cells. Thus, PTPφ expression is highest in quiescent macrophages, yet its relative subcellular distribution when examined by immunofluorescence does not change (data not shown). Since the proliferative rate of nontransformed cells decreases in cultures approaching confluence, we measured the expression of PTPφ in BAC1.2F5 cell cultures of various densities. Figure 2B demonstrates that expression of both the 43- and 47-kDa isoforms of PTPφ increased commensurate with cell density throughout log-phase growth, with the highest levels of expression detected in confluent cultures.

Overexpression of WT or C325S PTPφ does not affect macrophage proliferation or survival or cell density at confluence. To determine the function of the membrane-spanning isoforms of PTPφ in macrophages, the pLXSN retroviral vector was used to infect BAC1.2F5.2 cells with either the empty vector, a construct encoding the WT 47-kDa membrane-spanning isoform of PTPφ (WT PTPφ), or a construct encoding a catalytically inactive mutant of PTPφ (C325S PTPφ). Levels of PTPφ expression were determined by Western blotting (Fig. 2C). Subclones expressing the highest levels of PTPφ were selected for further characterization.

Since cell culture density affected PTPφ expression, growth and survival curves were carried out using one subclone each for control macrophages and those overexpressing either WT or C325S PTPφ. Despite slight variations in initial cell numbers seeded or plating efficiency of the cell lines, in the presence of CSF-1 the proliferative rates of cells overexpressing either WT or C325S PTPφ were not significantly different from those of control cells infected with the empty vector (Fig. 2D) and were comparable to the rate of proliferation of parental BAC1.2F5 cells (30). Furthermore, there was no detectable difference in cell density at confluence between the different infected cell lines. Likewise, alteration of PTPφ expression did not affect the ability of macrophages to survive in the absence of CSF-1 (Fig. 2E).

Overexpression of WT or C325S PTPφ alters macrophage morphology. The most striking differences noted between control cell lines containing the vector alone and cells overexpressing either WT or C325S PTPφ were morphological. The morphological differences were consistent between control cells (vectors 1 and 4), between cells overexpressing WT PTPφ (WT PTPφ 1, 4, and 18), and between cells overexpressing C325S PTPφ (C325S PTPφ 4, 8, and 15). WT PTPφ 1 and C325S PTPφ 8 were selected for subsequent morphological investigations because they expressed closer to upregulated endogenous levels of the WT protein and the highest levels of the mutant protein, respectively. As previously described (9), BAC1.2F5.2 control cells, in the presence of CSF-1, tended to be bipolar and well spread, with a leading edge and a trailing uropodium (Fig. 3a and g). When CSF-1 was removed for 24 h, these cells were rounded up and had retracted their pseudopodia (Fig. 3b and h). In contrast, cell lines overexpressing WT PTPφ, cultured in the presence of CSF-1, resembled CSF-1-starved control cells (Fig. 3b and c). Under scanning EM, the surface of
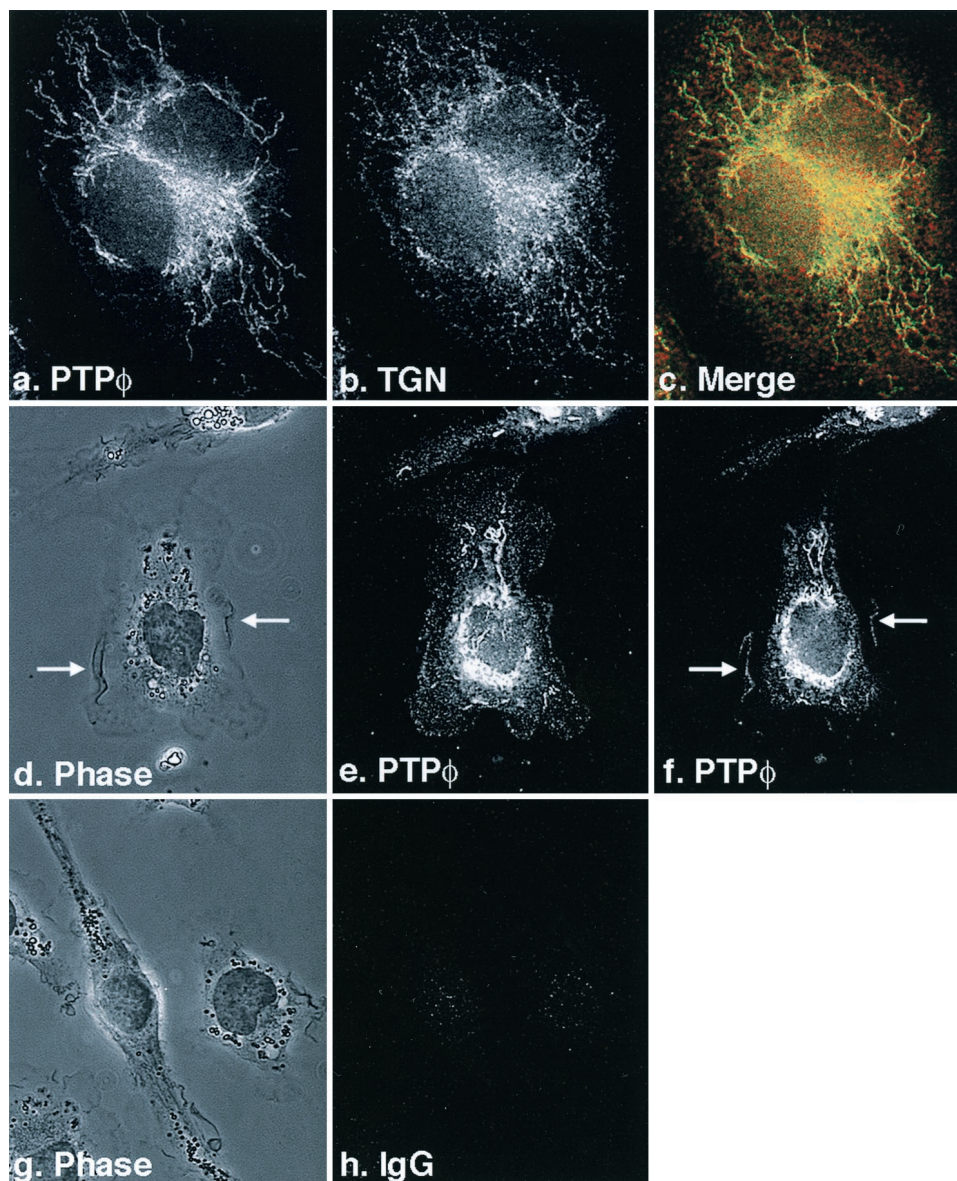
FIG. 1. Subcellular localization of PTPφ in BAC1.2F5 cells. Cells were cultured on fibronectin-coated glass coverslips and examined by immunofluorescence microscopy (a to c, e, f, and h) or by phase-contrast microscopy (d and g) at 100× magnification (a to c) or at 60× magnification (d to h), and images were recorded with an Olympus cooled CCD camera. Cells were immunostained with anti-C-terminal PTPφ (a, e, and f) or TGN38 (b) antibodies or IgG (h). Images in a and b were merged in c. The plane of focus was raised from e to f and arrows indicate dorsal ruffles in d and f.

these cells was shown to be roughened, displaying increased numbers of rudimentary ruffles but very few lamellipodia (Fig. 3h and i). Opposite effects were noted in cells overexpressing C325S PTPφ, which did not retract their pseudopodia markedly and continued to remain spread, with a smooth cell surface following removal of CSF-1 (Fig. 3e, f, k, and l). Thus, a consistent pattern was demonstrated that was reiterated in all of the subsequent morphology experiments: cells overexpressing WT PTPφ in the presence of CSF-1 resembled CSF-1-starved control cells, while cells overexpressing C325S PTPφ in the absence of CSF-1 resembled control cells in the presence of CSF-1.

Overexpression of WT or C325S PTPφ alters focal complex number and tyrosine phosphorylation content in macrophages. As shown above, the most obvious effects of altered PTPφ expression in macrophages were morphological. Since the increase in dorsal ruffling seen in cells overexpressing WT PTPφ suggested an adhesion defect, we examined the focal complex structure of the cell lines. Using an antibody directed to phosphotyrosine, immunofluorescent staining revealed that focal complexes in control macrophages cultured in CSF-1 were moderate in number and most prominently displayed around the periphery of cells (Fig. 4a). Upon removal of CSF-1, the number of focal complexes was decreased by 50%
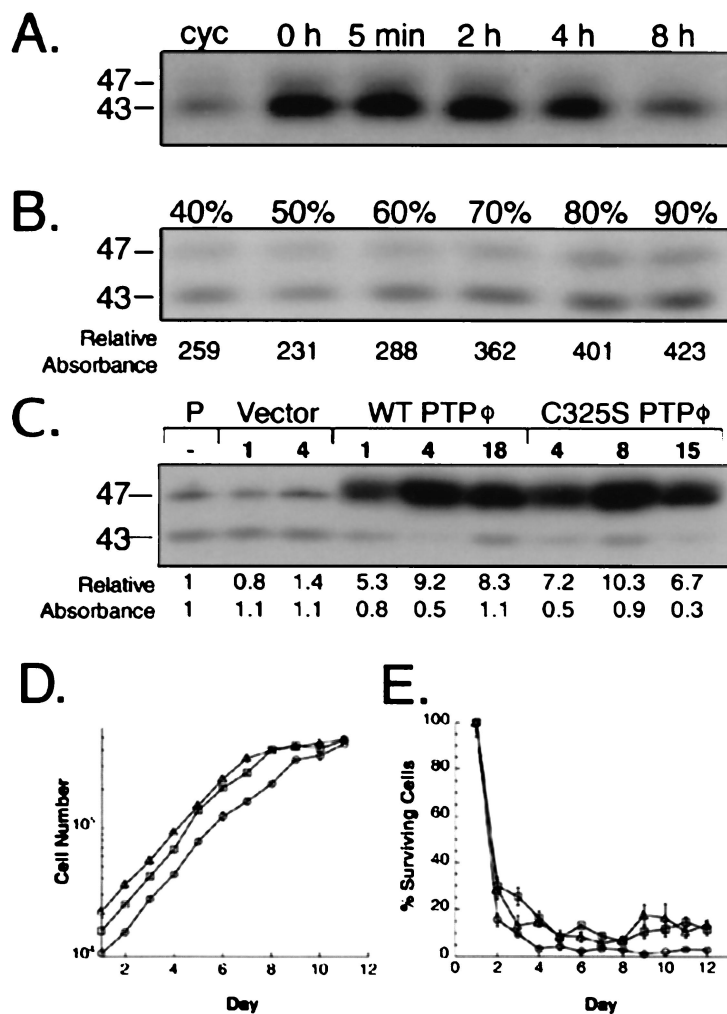
FIG. 2. Endogenous PTPφ expression is regulated by CSF-1 and affected by cell density, but alteration of PTPφ expression does not alter the rate of macrophage growth or survival. (A) Anti-PTPφ Western blot of NP-40-soluble lysates of BAC1.2F5 cells rendered quiescent by 24 h of incubation in the absence of CSF-1 and incubated with the growth factor for the indicated times. Cycling cells (cyc) were grown in the continuous presence of CSF-1. (B) Anti-PTPφ Western blot of NP-40-soluble lysates from BAC1.2F5 cells initially plated at 40% confluence and harvested daily until fully confluent. (C) Western blot of NP-40-soluble lysates from BAC1.2F5.2 parental cells (P) or stable, cloned cell lines which were retrovirally infected with either the empty vector, WT PTPφ, or phosphatase-inactive C325S PTPφ. The relative intensities of both the 43- and 47-kDa bands in B and C were determined densitometrically and are shown beneath the panels. (D) Growth (+CSF-1) and (E) survival (−CSF-1) curves for the different retrovirally infected BAC1.2F5.2 subclones. Square, vector; triangle, WT PTPφ; circle, C325S PTPφ. Error bars represent SEMs. Sizes are shown in kilodaltons in this and subsequent figures.

(Fig. 4b and g), as was the tyrosine phosphorylation content of the remaining focal complexes, as measured by mean pixel intensity (Fig. 4h). Consistent with the morphological findings, cells overexpressing WT PTPφ displayed reduced numbers and tyrosine phosphorylation levels of focal complexes in the presence of CSF-1 (Fig. 4c, g, and h), while cells overexpressing C325S PTPφ contained striking focal complexes that persisted upon removal of CSF-1 (Fig. 4e to h). Staining of focal complexes using antibodies to two other focal contact proteins, β1 integrin and vinculin, demonstrated a similar disruption of focal contact numbers (data not shown). These results indicate that increased expression of PTPφ in either CSF-1-starved control cells or WT PTPφ-overexpressing cells disrupts focal complexes.

PTPφ-induced focal complex disruption affects the actin cytoskeleton in a CSF-1-dependent manner. F-actin stress fibers arising from focal contacts in fibroblasts have been well documented, but actin bundles were not detected to originate from the less well-organized focal complexes in macrophages (2). Using the more sensitive cooled CCD microscopy, however, we were able to demonstrate that longer and larger microfilament bundles, while never substantial enough to constitute stress fibers like those seen in fibroblasts, sometimes arose from well-defined focal complexes in control cells stained for antiphosphotyrosine to highlight focal complexes and TRITC-phalloidin to detect F-actin (Fig. 5a and b). F-actin staining in control cells showed moderate numbers of actin bundles, especially extending into pseudopodia (Fig. 5c). If CSF-1 was removed from these cells for 24 h, the actin bundles frequently disappeared altogether (Fig. 5d). In cell lines overexpressing WT PTPφ, few actin bundles were visible, even in the presence of CSF-1 (Fig. 5e and f), while cells overexpressing C325S
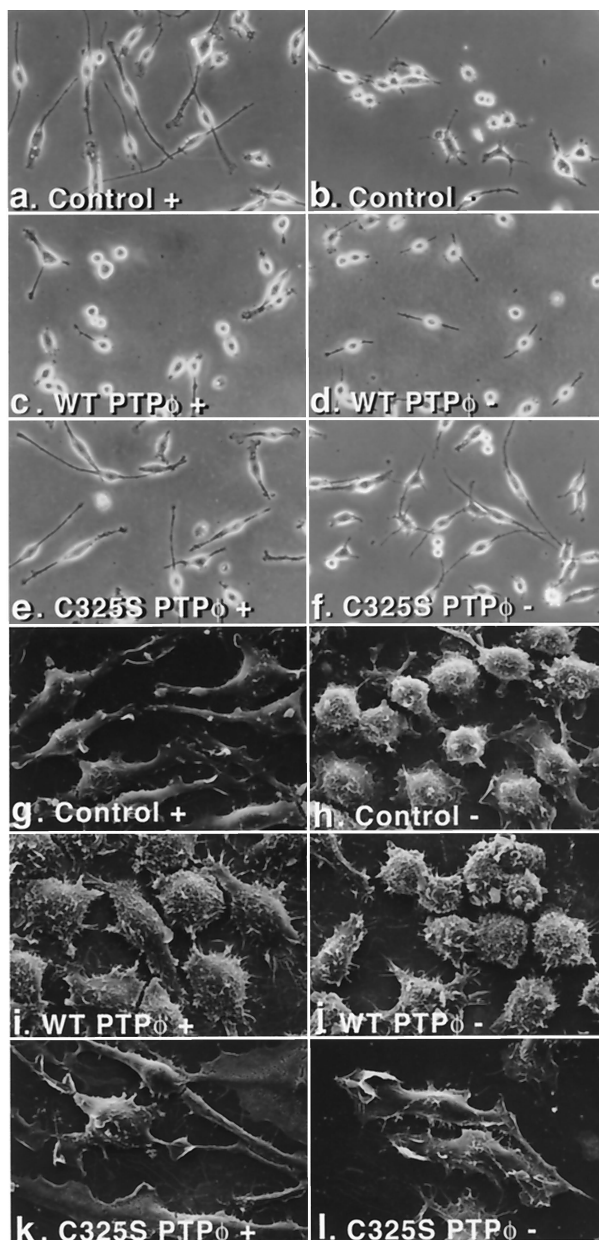
FIG. 3. Effect of alteration of PTPφ expression on macrophage morphology. Macrophage cell lines containing the empty vector control (a, b, g, and h) or overexpressing either WT PTPφ (c, d, i, and j) or C325S PTPφ (e, f, k, and l) were plated on tissue culture plates and cultured either in the presence (+, left panels) or absence (−, right panels) of CSF-1 and examined live, using phase-contrast microscopy at 200× magnification (a to f), or fixed, using scanning EM at 1,500× magnification (g to l).

PTPφ, in the absence of CSF-1, retained many actin bundles (Fig. 5g and h). Morphometric quantitation of actin bundle numbers confirmed these differences (Fig. 5i), and the findings are in keeping with the demonstrated alterations in focal complex numbers and cell morphology upon overexpression of either WT or C325S PTPφ. However, we found no differences in either total cell F-actin by N-(7-nitrobenz-2-oxa-1,3-diazol-4-yl)phallacidin assay (13) or the relative distribution of F-actin cross-linked into the cytoskeleton by differential centrif-

ugation (18) (data not shown). These results are consistent with the fact that actin bundles comprise a small proportion of total cell F-actin and that the altered morphology induced by increased PTPφ expression was not due to substantial changes in cellular F-actin. There were no differences in the microtubular cytoskeletons of the different cell lines, as demonstrated using immunofluorescent staining for β-tubulin (results not shown).
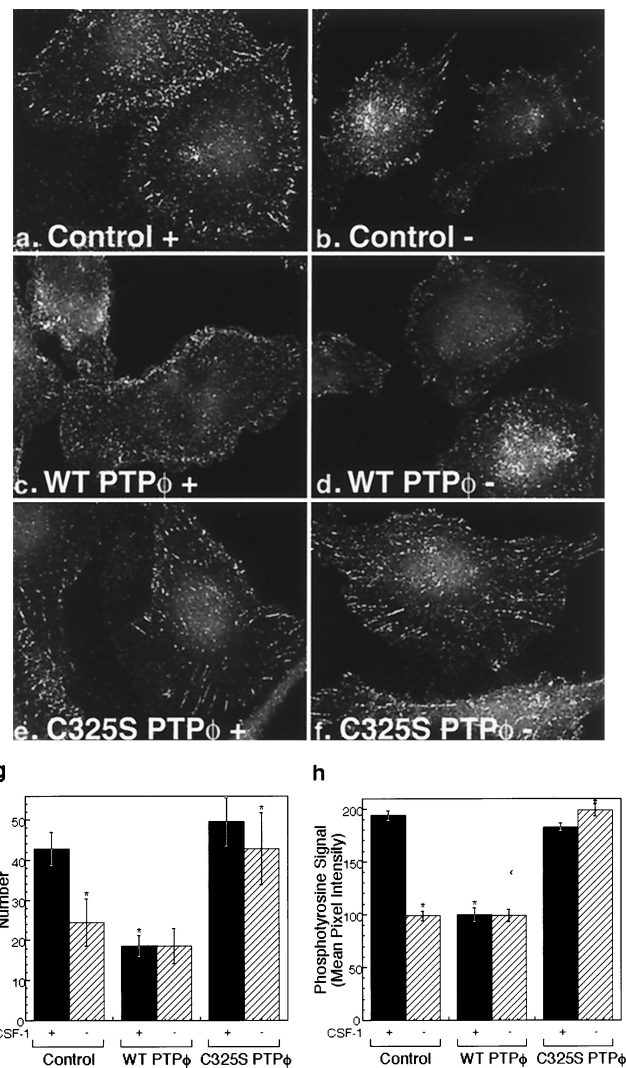

FIG. 4. Focal complexes are reduced in number and phosphotyrosine content upon removal of CSF-1 or with overexpression of WT PTPφ. Immunofluorescent staining of phosphotyrosine in focal complexes in cells containing the empty vector (a and b) or overexpressing either WT PTPφ (c and d) or C325S PTPφ (e and f) in the presence (a, c, and e) or absence (b, d, and f) of CSF-1 was examined at 60× magnification. Focal complex numbers (g) and tyrosine phosphorylation content (h) were quantitated for the different cell lines in the presence (solid bars) and absence (hatched bars) of CSF-1. Error bars represent (g) SD and (h) SEM. Analysis of variance (ANOVA) testing for differences in the means was highly significant ($P < 0.0001$). The following comparisons were significant ($P < 0.01$) by Bonferroni's selected t test: control with and without CSF-1, control and C325S PTPφ compared with WT PTPφ in the presence of CSF-1, and control and WT PTPφ compared with C325S PTPφ in the absence of CSF-1, $n > 250$.
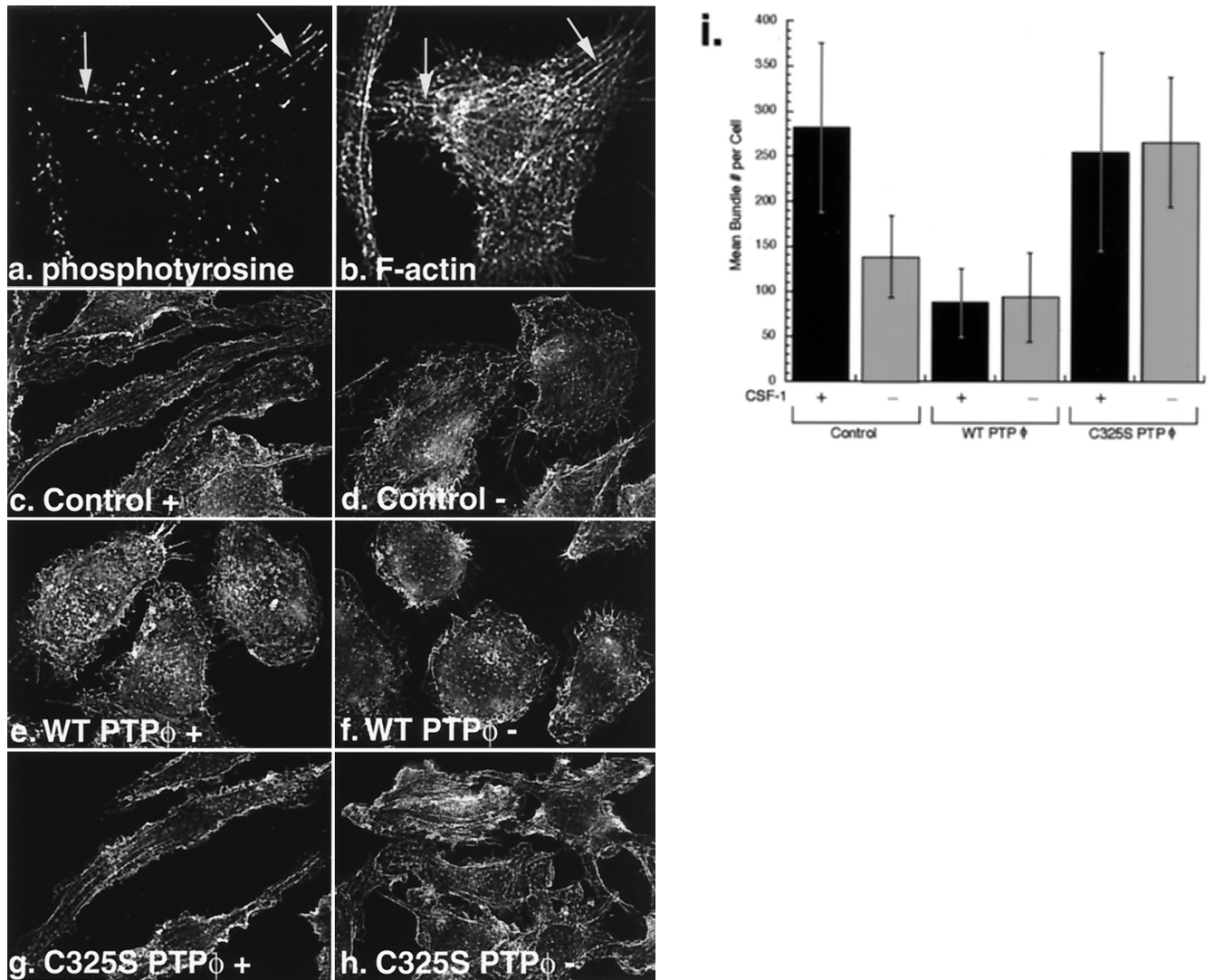
FIG. 5. Actin bundles sometimes arise from focal complexes in macrophages and are reduced in number by increased PTPφ expression. Macrophage cell lines containing the empty vector (a to d) or overexpressing either WT PTPφ (e and f) or C325S PTPφ (g and h) were plated on glass coverslips and cultured either in the presence (a, b, c, e, and g) or absence (d, f, and h) of CSF-1. Cells were fixed, stained for antiphosphotyrosine (a) or F-actin (b to h), and examined by immunofluorescence microscopy at 60× magnification. Arrows indicate focal complexes from which actin bundles can be seen to arise (a and b). Quantitative morphometric analysis of F-actin bundle numbers is graphically illustrated in i, with cells grown in the presence (solid bars) and absence (shaded bars) of CSF-1. Error bars represent SD. ANOVA testing for differences in the means was highly significant ($P < 0.001$). The following comparisons were significant ($P < 0.01$) by Bonferroni's selected t test: control with and without CSF-1, control, and C325S PTPφ compared with WT PTPφ in the presence of CSF-1, and control and WT PTPφ compared with C325S PTPφ in the absence of CSF-1, $n = 25$.

Macrophage adhesion is decreased and motility increased by increased PTPφ expression. Since increased expression of WT PTPφ leads to focal complex disruption in macrophages, we measured adhesion of the different cell lines as a biological assay of focal complex integrity. Macrophages adhere to and spread more readily on fibronectin than laminin (Fig. 6a and b), consistent with a more flattened morphology seen on fibronectin in all cell lines (data not shown). Consequently, any differences in the ability of the various cell lines to adhere to fibronectin were difficult to detect consistently. In contrast, the reduced ability of macrophages to adhere to laminin allowed the detection of significant differences between cells expressing C325S PTPφ, 40% of which remained adherent; control cells,

10% of which were adherent; and cells overexpressing WT PTPφ, less than 5% of which were adherent 45 min after plating. These differences were largely unchanged at 2 h and indicate that increased PTPφ decreases macrophage adhesion (Fig. 5a and b). Since cells overexpressing C325S PTPφ were not significantly better spread at 45 min than cells overexpressing WT PTPφ (data not shown), adherence rather than spreading was contributing to this phenotype.

Decreased adhesion can stimulate or inhibit cell motility (29). To determine how alteration of PTPφ expression influenced macrophage motility, the cell lines were subjected to a wound-healing assay. Macrophages overexpressing WT PTPφ migrated more rapidly and macrophages expressing C325S
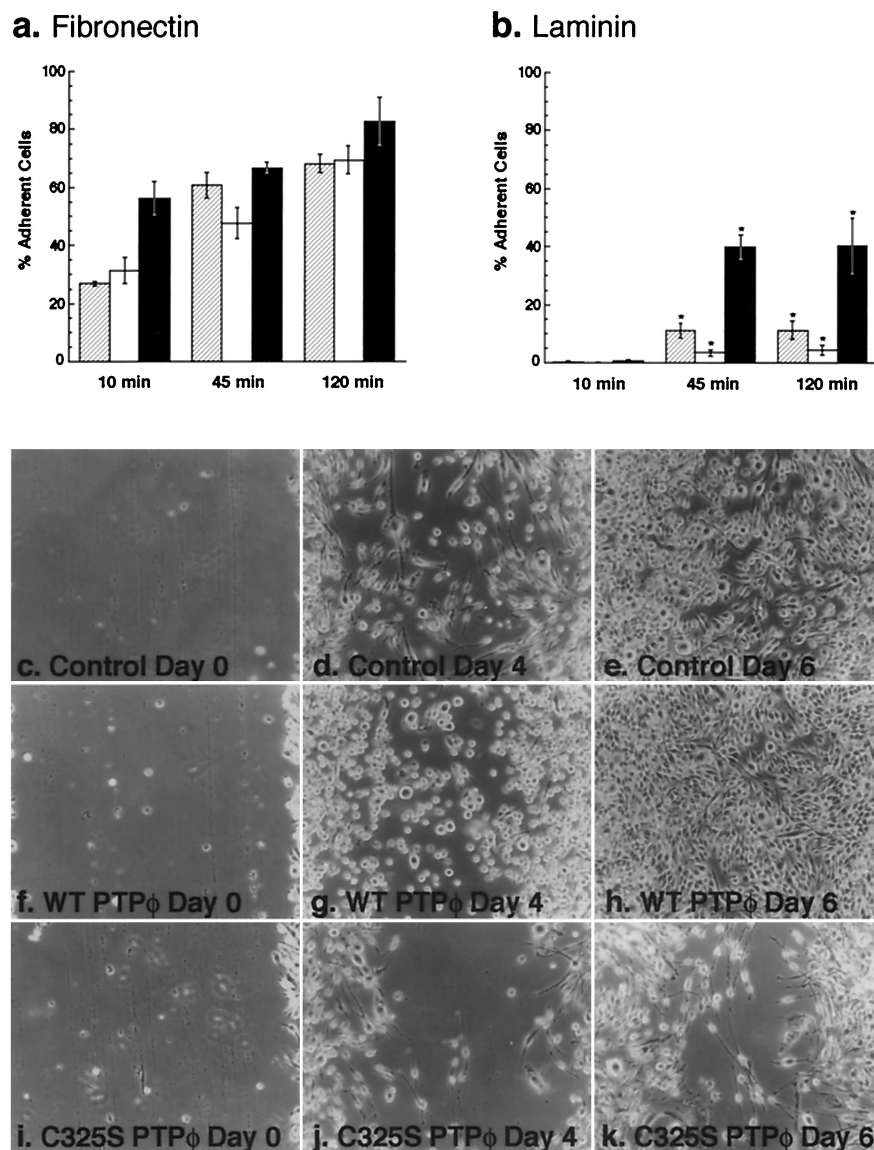
a. Fibronectin

b. Laminin

FIG. 6. Alteration of PTPφ expression affects macrophage adhesion on laminin and motility. (a and b) Adhesion assay. Cells were scraped and replated on fibronectin (a) or laminin (b) for the indicated times, then washed and fixed, and adherent cells were counted (control, hatched; WT PTPφ, white; C325S PTPφ, solid). Error bars represent SEM. ANOVA testing for differences in the means was highly significant for laminin ($P < 0.0001$). The following comparisons were significant ($P < 0.01$) by Bonferroni's selected t test: control compared with WT PTPφ and control compared with C325S PTPφ at both 45 and 120 min (asterisked in b). (c to k) Wound-healing assay. Cells were grown to confluence on tissue culture plastic, the monolayers were scored to create a wound, and the cultures were fed daily and photographed live as the wound healed (100×). Control cells (c to e), cells overexpressing WT PTPφ (f to h), and cells expressing C325S PTPφ (i to k) were photographed at 0, 4, and 6 days. (The slow wound healing is probably contributed to by the following. [i] In contrast to fibroblasts, macrophage migration into a wound is a random process. [ii] Macrophages cultured in homogeneous CSF-1 rather than a CSF-1 gradient lose polarity [45]. [iii] BAC1.2F5 cells migrate more slowly than primary macrophages [K. Berg and F. J. Pixley, unpublished observations]).

PTPφ migrated more slowly into the defect than control macrophages (Fig. 6c to k). Preliminary studies using time-lapse videomicroscopy also demonstrate increased velocity of cell motility in cells overexpressing WT PTPφ and reduced motility in cells overexpressing C325S PTPφ (data not shown). Thus, increased levels of PTPφ increase cell motility as a result of focal complex disruption. This result is in keeping with findings in neutrophils, which indicated that a lack of strongly adherent focal contacts was important for these cells to respond rapidly to chemotactic agents or to engulf particles (25).

PTPφ is not found in focal complexes but colocalizes with paxillin and Pyk2 in dorsal ruffles. Increased PTPφ expression leads to a decrease in the number and phosphotyrosine content of focal complexes. To determine whether this effect was due to a direct action of PTPφ within focal complexes, we carried out dual immunofluorescent staining of PTPφ and focal complexes by antiphosphotyrosine. We were unable to detect any PTPφ in focal complexes, even in cells overexpressing C325S PTPφ (Fig. 7a and c). Indeed, at the optimal plane of focus for the detection of focal complexes by antiphosphotyrosine stain-
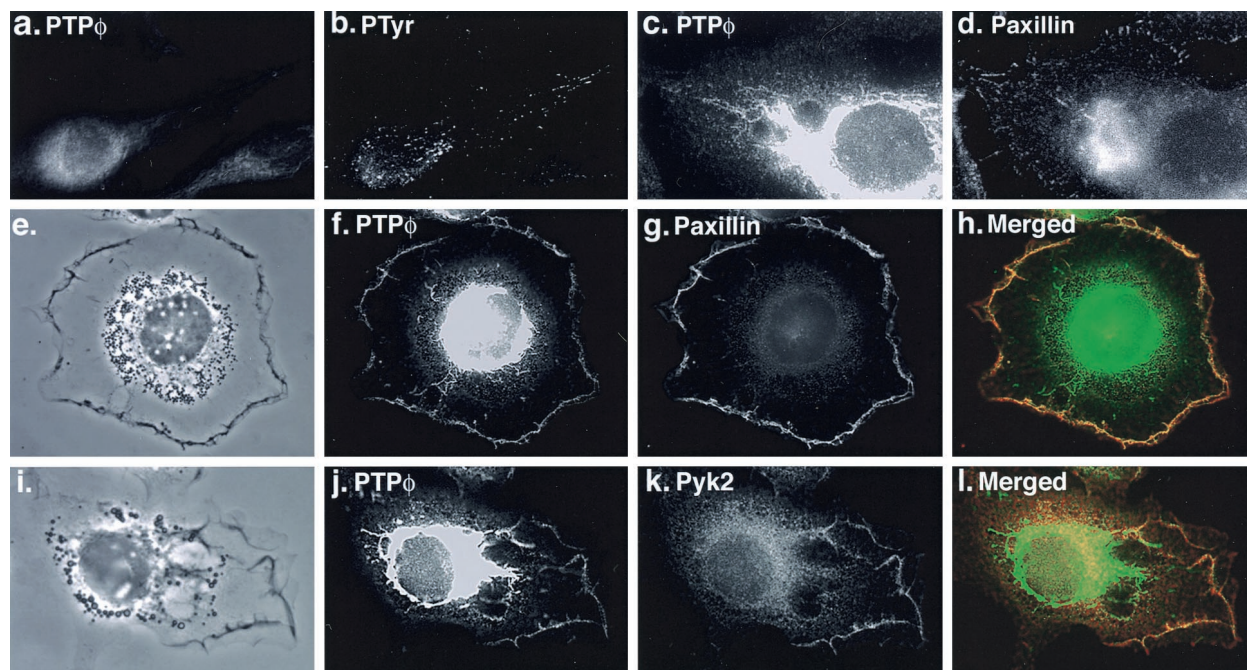
FIG. 7. PTPϕ does not localize to focal complexes yet it colocalizes with paxillin and Pyk2 in dorsal ruffles. Immunofluorescent staining of PTPϕ (a) demonstrates that it does not colocalize with phosphotyrosine in focal complexes (b) in cells expressing C325S PTPϕ. Neither does PTPϕ (c) colocalize with paxillin (d) in focal complexes but it does colocalize with paxillin (e to h) and Pyk2 (i to l) in dorsal ruffles.

ing, PTPϕ staining was difficult to demonstrate (Fig. 7a to d). It is possible that PTPϕ could indirectly disrupt focal complex formation by regulating changes in integrin expression. However, Western blot analysis of the relative expression levels of the broadly expressed β1 and α4 integrins and the leukocyte-restricted β2 integrin showed no significant differences in expression levels in all three cell lines (data not shown).

A major tyrosine-phosphorylated component of focal complexes is paxillin (Fig. 7d) (44), and tyrosine-phosphorylated paxillin is also found at the periphery of the cell (31). Since PTPϕ is present in dorsal ruffles (Fig. 1d and f), its potential colocalization with paxillin in these structures was examined. C325S PTPϕ-expressing cells stimulated with CSF-1 for 5 min were used to maximize detection of both tyrosine phosphorylation and dorsal ruffles, respectively (9, 47). PTPϕ was shown to colocalize with paxillin in every dorsal ruffle examined (Fig. 7e to h) but not in focal complexes (Fig. 7c and d). Paxillin has also been shown to colocalize with Pyk2 in dorsal ruffles of BAC1.2F5 macrophages (46). Immunofluorescent staining of PTPϕ and Pyk2 showed a similar colocalization (Fig. 7j to l). Thus, although PTPϕ does not colocalize with paxillin in focal complexes, it colocalizes with paxillin and Pyk2 in dorsal ruffles.

Focal complex paxillin levels are inversely correlated with the levels of PTPϕ. Since paxillin is a major contributor of focal complex tyrosine phosphorylation, we examined the level of paxillin in the focal complexes of the different cell lines using immunofluorescence. The level of paxillin was more severely reduced than the level of tyrosine phosphorylation in the focal complexes in cells overexpressing WT PTPϕ (Fig. 8e to h) compared with control cells (Fig. 8a to d) and cells expressing C325S PTPϕ (Fig. 8i to l). These effects were again most

clearly demonstrated in WT PTPϕ-overexpressing cells in the presence of CSF-1 (Fig. 8e and f) and CSF-1-starved C325S PTPϕ-overexpressing cells (Fig. 8k and l). Quantitation of mean pixel intensities for paxillin-stained focal complexes was shown to be significantly reduced in cells overexpressing WT PTPϕ, in the presence and absence of CSF-1, and in control cells upon removal of CSF-1, while cells expressing C325S PTPϕ had the same levels of paxillin in their focal complexes in the presence or absence of CSF-1 as control cells in the presence of CSF-1 (Fig. 8m). The reduction in the paxillin signal of cells overexpressing WT PTPϕ by approximately 90% (Fig. 8m) is significantly greater than the ~55% reduction in the phosphotyrosine signal in the same cells (Fig. 4h). This selective depletion of paxillin from focal complexes is reflected in the ratio of paxillin to phosphotyrosine signals for the three cell lines (Fig. 8n) and was confirmed by demonstrating that the ratios of paxillin to β1 integrin staining paralleled the paxillin/phosphotyrosine ratios (data not shown). Additionally, while staining for vinculin demonstrated the expected disruption in focal complex numbers upon increased expression of WT PTPϕ, there were no differences in the strength of the vinculin signal in individual focal complexes of the cell lines (mean signal ± standard error of the mean [SEM]: control, 151.1 ± 4.9; WT PTPϕ, 150.8 ± 3.8; and C325S PTPϕ 146.8 ± 4.0). Thus, despite the absence of detectable PTPϕ within macrophage focal complexes, its expression is inversely correlated with the incorporation of paxillin into focal complexes.

Paxillin tyrosine phosphorylation is specifically regulated by PTPϕ. To determine whether paxillin tyrosine phosphorylation is regulated by PTPϕ, paxillin immunoprecipitation of NP-40-soluble cell lysates of the cell lines, cycling in the presence of CSF-1, was carried out, followed by SDS-PAGE and
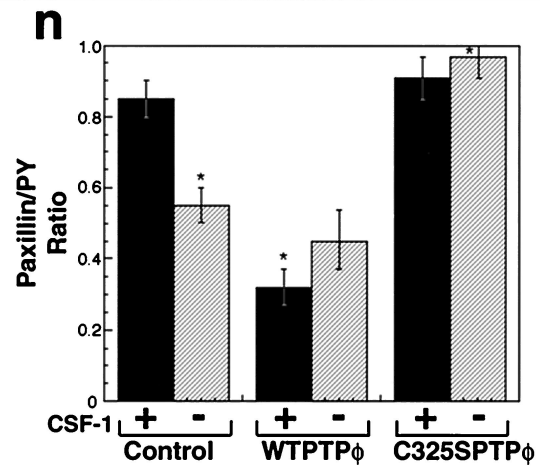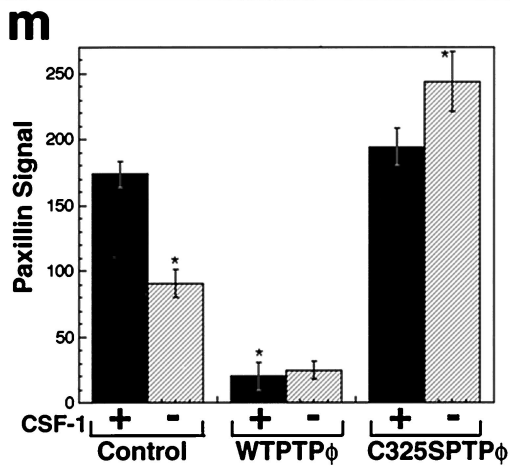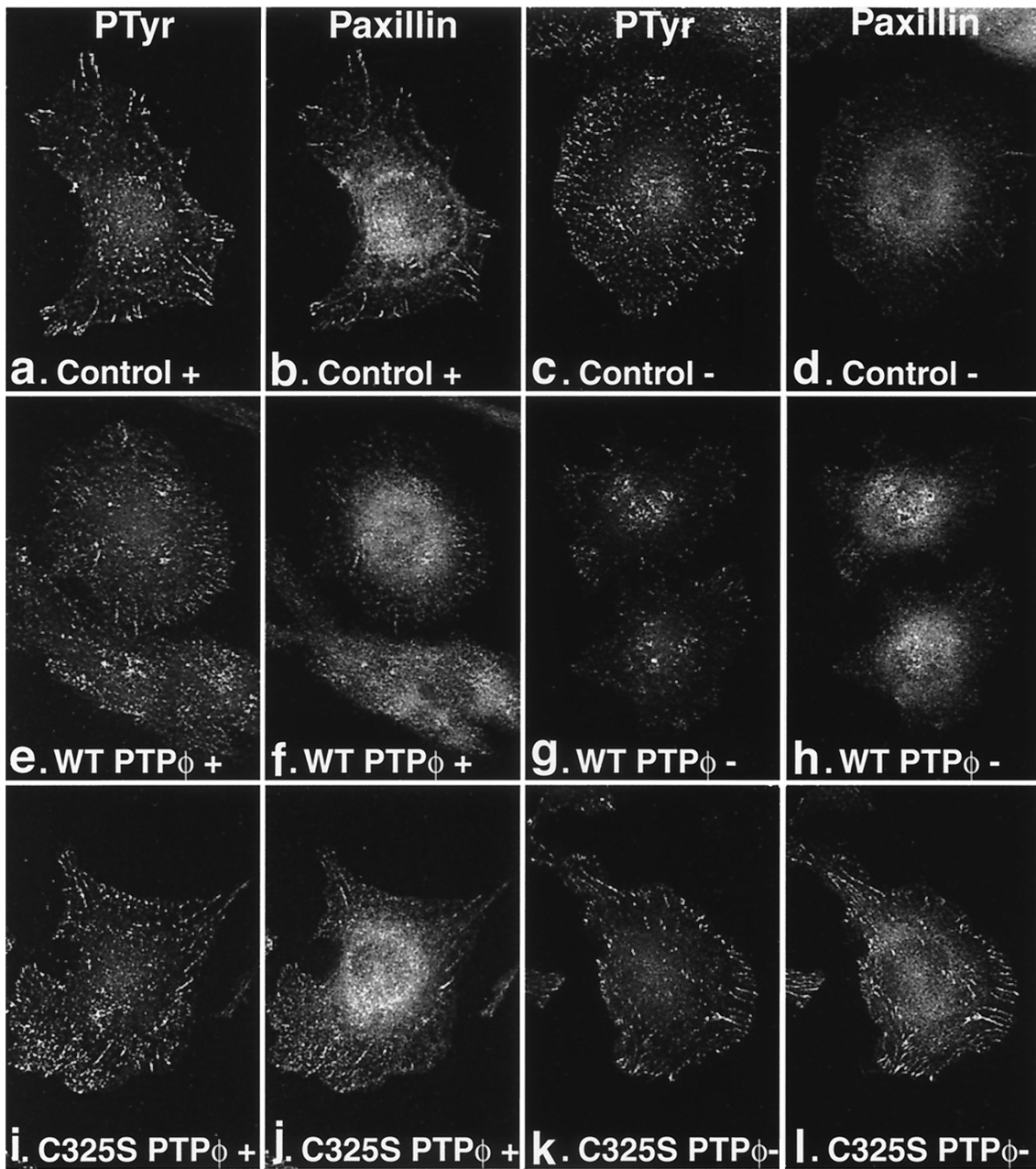
Western blotting analysis. Paxillin tyrosine phosphorylation was significantly decreased in cells overexpressing WT PTPφ and markedly increased in cells overexpressing C325S PTPφ (Fig. 9A). When the same lysates were subjected to Pyk2 and FAK immunoprecipitation, neither protein was significantly tyrosine phosphorylated in any of the cell lines (Fig. 9A). In CSF-1-starved parental BAC1.2F5 cells exhibiting an increase in PTPφ expression, tyrosine phosphorylation levels of paxillin were also decreased, while total-cell paxillin levels were not altered (data not shown). Paxillin was shown to coimmunoprecipitate significant amounts of Pyk2, as has been shown previously in BAC1.2F5 macrophages (46), and small amounts of paxillin were coimmunoprecipitated with Pyk2 (Fig. 9A). Subsequent immunoprecipitations have shown that the association of Pyk2 with paxillin is phosphotyrosine independent (data not shown), as has been demonstrated in other cell types (36). The Pyk2-related tyrosine kinase FAK was expressed at very low levels and was not shown to associate with paxillin (Fig. 9A). Since Pyk2 tyrosine phosphorylation was almost undetectable in cycling cells (Fig. 9A), its tyrosine phosphorylation was examined in cells that were stimulated with CSF-1 for 15 min, conditions yielding maximal Pyk2 tyrosine phosphorylation. There was no difference in the degree of Pyk2 phosphorylation among the three cell lines under these conditions (Fig. 9B). Similarly, there were no differences between the three cell lines in the degree of tyrosine phosphorylation of the CSF-1R (Fig. 9C) or in the pattern of tyrosine phosphorylation in antiphosphotyrosine immunoprecipitates (Fig. 9D) when cells were stimulated by CSF-1 for 2 min (Fig. 9C) and 15 min (Fig. 9D), respectively, to maximize tyrosine phosphorylation levels of the observed proteins (there was no tyrosine phosphorylation of the CSF-1R without stimulation). These results demonstrate that paxillin is selectively dephosphorylated by PTPφ in vivo.

PTPφ is associated with paxillin and Pyk2. Initial phosphotyrosine and paxillin Western blotting of PTPφ immunoprecipitates from all three cell lines after stimulation with CSF-1 for 15 min failed to demonstrate any consistent coimmunoprecipitation of paxillin (Fig. 9E). Instead, PTPφ immunoprecipitates consistently demonstrated constitutive association of PTPφ with Pyk2 (Fig. 9E). However, when paxillin tyrosine phosphorylation levels were significantly increased by pervanadate treatment of the cells for 10 min before lysis, paxillin as well as Pyk2 could be demonstrated in PTPφ immunoprecipitates (Fig. 9E), indicating that these three proteins can exist in a complex in vivo.

Catalytic domain of C325S PTPφ preferentially binds paxillin in vitro. Of the two identified PTPφ-associated proteins, only paxillin was shown to be dephosphorylated by PTPφ in vivo (Fig. 9A and B). To determine whether there was a direct interaction between PTPφ and paxillin, the antiphosphotyro-

sine immunoprecipitate blot (Fig. 9D) was stripped and subjected to Far Western analysis with a GST-C325S PTPφ catalytic domain fusion protein. The mutant PTPφ catalytic domain did not detectably bind any phosphotyrosyl proteins (data not shown), suggesting that the association between PTPφ and its substrate(s) is of low affinity or that association is not possible following SDS-PAGE and renaturation. To optimize detection of an interaction, whole-cell lysates of pervanadate-treated, CSF-1-stimulated C325S PTPφ-overexpressing cells were incubated with immobilized GST-PTPφ catalytic domain fusion proteins. Bound proteins were eluted and subjected to SDS-PAGE and Western blotting analysis with antiphosphotyrosine, antipaxillin, anti-Pyk2, and anti-GST-PTPφ antibodies (Fig. 10). Several proteins were selectively bound by GST-PTPφ catalytic domain proteins. The most highly tyrosine phosphorylated of these protein bands were the three bands that comigrated with three of the paxillin bands detected by Western blotting (Fig. 10A and B). Pyk2 was also selectively bound and comigrated with a resolvable but faintly tyrosine-phosphorylated band (Fig. 10A and B). The mutant PTPφ catalytic domain bound more paxillin and Pyk2 than the WT catalytic domain. The low catalytic activity of WT PTPφ for bound paxillin is likely due to the presence of orthovanadate in the binding and wash buffers. Importantly, the ratio of paxillin to Pyk2 bound to PTPφ in vitro was much higher than the paxillin/Pyk2 ratio in Pyk2 immunoprecipitates from C325S PTPφ-expressing cells (Fig. 9A), consistent with an additional interaction between the PTPφ-catalytic site and paxillin, independent of Pyk2. Western blotting with anti-p130^{cas} antibodies did not show any p130^{cas} bound to the PTPφ catalytic domain (data not shown). This experiment indicates that the catalytic domain of PTPφ selectively binds paxillin and Pyk2. Use of a D291A PTPφ "substrate-trapping" mutant did not significantly increase the ability of the catalytic domain to bind paxillin or Pyk2 (data not shown).

DISCUSSION

By overexpressing either the WT or a phosphatase-inactive form of PTPφ in BAC1.2F5 macrophages, we have shown that PTPφ mediates CSF-1-regulated changes in macrophage morphology without affecting proliferation or survival. It effects these morphological changes by disrupting focal complex formation. This disruption is accompanied by tyrosine dephosphorylation of paxillin and a decrease in the paxillin concentration in focal complexes. PTPφ is associated with paxillin and Pyk2 in vivo and selectively binds paxillin and Pyk2 in vitro, yet it does not affect Pyk2 tyrosine phosphorylation levels. Relative amounts of paxillin and Pyk2 bound to PTPφ from the in vivo and in vitro experiments indicate that the interaction between PTPφ and pax-

FIG. 8. Paxillin is selectively depleted in focal complexes by overexpression of WT PTPφ. Immunofluorescent staining of focal complexes in control cells (a to d), cells overexpressing WT PTPφ (e to h), and cells expressing C325S PTPφ (i to l) in the presence (+) and absence (−) of CSF-1 using antiphosphotyrosine (a, c, e, g, i, and k) and antipaxillin (b, d, f, h, j, and l) antibodies. Absolute pixel intensity for paxillin staining in the focal complexes of the different cell lines (m) and relative pixel intensity for paxillin staining compared with phosphotyrosine (PTyr) staining (n) were quantitated. Both sets of data were calculated in the presence (solid bars) or absence (hatched bars) of CSF-1. Error bars represent SEM (m and n). ANOVA testing for differences in means was highly significant ($P < 0.0001$). The following comparisons were significant ($P < 0.01$) by Bonferroni's selected t test: control with and without CSF-1, control, and C325S PTPφ compared with WT PTPφ in the presence of CSF-1, and control and WT PTPφ compared with C325S PTPφ in the absence of CSF-1, $n = 50$. Cells overexpressing WT PTPφ were selected to display better than average focal complexes in order to demonstrate paxillin staining in their focal complexes.
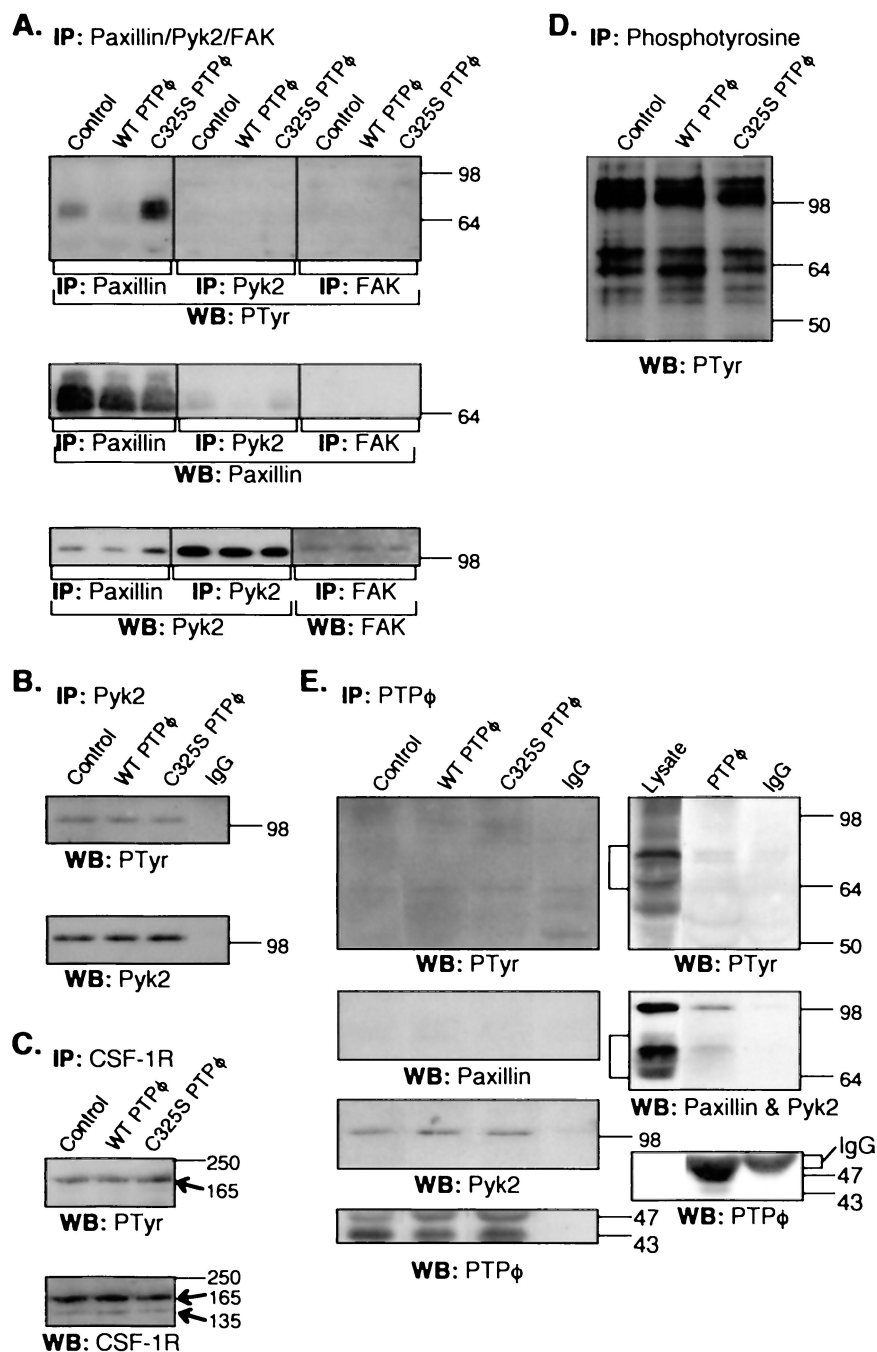
FIG. 9. PTPφ specifically modulates paxillin phosphorylation in vivo and associates with paxillin and Pyk2. Control macrophages, macrophages overexpressing WT PTPφ, and macrophages overexpressing C325S PTPφ were grown continuously in the presence of CSF-1 (A) or were starved of CSF-1 for 24 h and then CSF-1-stimulated for either 15 min (B, D and E) or 2 min (C). NP-40-soluble lysates were subjected to the following immunoprecipitations (IP) and Western blotting (WB). (A) antipaxillin, anti-Pyk2, and anti-FAK immunoprecipitates were blotted with anti-PTyr, -paxillin, -Pyk2, and -FAK Abs. B Anti-Pyk2 immunoprecipitates were blotted with anti-PTyr and -Pyk2 Abs. C Anti-CSF-1R immunoprecipitates were blotted with anti-PTyr and -CSF-1R Abs (arrows indicate the 165-kDa mature and 135-kDa precursor CSF-1R proteins). (D) Anti-PTyr immunoprecipitates were blotted with an anti-PTyr Ab. (E) Anti-PTPφ and IgG immunoprecipitates were blotted with anti-PTyr, -paxillin, -Pyk2, and -PTPφ Abs. Left panels, no pervanadate treatment. Right panels, pervanadate treatment was carried out for 10 min before cell lysis.

illin is of low affinity and that the interaction may be stabilized by the additional higher-affinity interaction between PTPφ and Pyk2. Thus, Pyk2 may be acting as a bridging molecule. The only subcellular site where these three proteins colocalize is in the dorsal ruffle, not the focal complex

in which paxillin is found. Taken together, these data suggest that PTPφ regulates focal complex formation by dephosphorylating paxillin in the dorsal ruffles, thereby reducing the amount of phosphorylated paxillin available for incorporation into focal complexes. As a consequence of
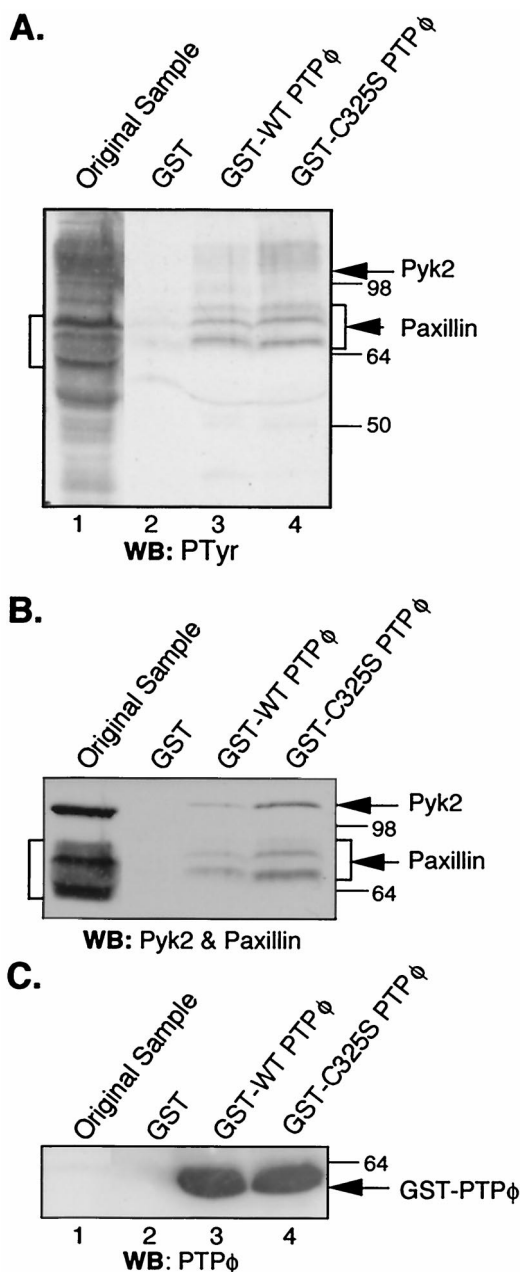
FIG. 10. Paxillin and Pyk2 preferentially bind to GST-C325S PTPϕ in vitro. NP-40-soluble lysates from CSF-1-stimulated, pervanadate-treated macrophages expressing C325S PTPϕ (lane 1) and proteins eluted from GST (lane 2), GST-WT PTPϕ (lane 3), and GST-C325S PTPϕ (lane 4) were subjected to (A) anti-PTyr, (B) mixed antipaxillin and anti-Pyk2, and (C) anti-PTPϕ Western blotting (WB). Sodium orthovanadate was used in the lysis and wash buffers. Arrows indicate Pyk2 and GST-PTPϕ. Paxillin protein bands are bracketed. The migration of the paxillin and Pyk2 bands was slower in the lanes containing the GST-PTPϕ fusion protein elutions (lanes 3 and 4) than in the lane with the original sample (lane 1) due to the large amount of eluted fusion protein. This push-up effect also slightly compressed the region covered by the paxillin bands.

increased PTPϕ expression, decreased paxillin tyrosine phosphorylation, and focal complex disruption, macrophages are less adherent and more motile.

PTPϕ mediates CSF-1-regulated changes in macrophage morphology, adhesion, and motility. CSF-1 starvation of mac-

rophages causes increased PTPϕ expression and results in cell rounding, pseudopodial retraction, and dorsal ruffling, changes mimicked by overexpression of PTPϕ (Fig. 3). It is not expected, a priori, that expression of a cysteine-to-serine PTP mutant will lead to dominant negative effects (42). However, the C325S mutant form of PTPϕ behaves in a dominant negative manner, causing macrophages to retain the spread morphology of cycling cells even after CSF-1 starvation. Consistent with these opposing effects of overexpression of WT and C325S PTPϕ, immunofluorescent staining revealed a gradation in number of focal complexes and their degree of tyrosine phosphorylation that is inversely proportional to the level of effective activity of PTPϕ.

As a result of the PTPϕ-induced disruption of focal complexes, macrophage adhesion was reduced and motility was increased. The large number of dorsal ruffles seen in quiescent macrophages and cells overexpressing WT PTPϕ is likely a response to reduced adhesion of lamellipodia to the ECM, causing them to be retracted as dorsal ruffles. This response has been noted frequently in cells that are detached from culture surfaces and placed in suspension and results from the action of retraction forces in the absence of strong adhesion (7). The ability of a cell to adhere to the ECM directly influences its ability to move (29), and motility studies in neutrophils emphasize the requirement for weakly adherent focal contacts in order for phagocytes to respond rapidly to chemotactic agents or to engulf particles (25). In macrophages, PTPϕ activity ensures that focal complexes are not too adherent and well organized. By disrupting focal complexes and thereby reducing adhesion, PTPϕ mediates the morphological and motility-stimulating effects of CSF-1.

Paxillin is a candidate substrate of PTPϕ in macrophages. Paxillin is a 68-kDa cytosolic protein that is phosphorylated on tyrosine and incorporated into focal contacts in response to the engagement of integrin receptors with the ECM or following growth factor stimulation (44). Results from several experiments indicate that paxillin is a substrate of PTPϕ. First, tyrosine phosphorylation of paxillin is reduced in cells overexpressing WT PTPϕ and increased in C325S PTPϕ-overexpressing cells. Second, compared with other tyrosine-phosphorylated proteins, paxillin is preferentially depleted from focal complexes in cells overexpressing WT PTPϕ. Furthermore, the tyrosine dephosphorylation by PTPϕ was specific in that there was no difference in the overall pattern of cellular protein tyrosine phosphorylation or in the tyrosine phosphorylation of the CSF-1R or Pyk2 tyrosine kinases between cells overexpressing WT and C325S PTPϕ. Third, PTPϕ associates with paxillin in vivo. Fourth, paxillin was the most strongly tyrosine-phosphorylated protein bound to the GST-PTPϕ catalytic domain fusion proteins in vitro and more was bound by GST-C325S PTPϕ than by GST-WT PTPϕ.

In vivo immunoprecipitation experiments indicate that PTPϕ, paxillin, and Pyk2 are associated in a complex. While we were unable to demonstrate direct association of paxillin or any other protein with PTPϕ by Far Western analysis, the altered ratio of paxillin and Pyk2 binding to PTPϕ demonstrated by the in vitro binding data is consistent with a direct interaction between paxillin and PTPϕ. The constitutive, phosphotyrosine-independent association of Pyk2 with both PTPϕ and paxillin indicates that Pyk2 may be acting as a bridging
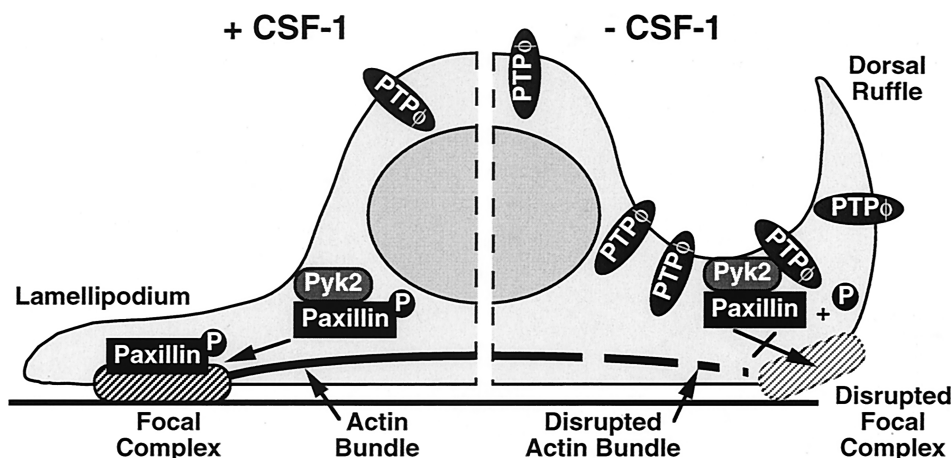
FIG. 11. Phosphotyrosyl paxillin incorporation model for the formation of focal complexes in macrophages. PTPφ and Pyk2, and paxillin and Pyk2 stably associate in macrophages. As indicated on the left side of the diagram, in the presence of CSF-1, baseline levels of PTPφ permit sufficient paxillin tyrosine phosphorylation for normal incorporation of phosphotyrosyl paxillin into focal complexes. In contrast, increased PTPφ levels in CSF-1-starved cells lead to dephosphorylation of paxillin, disrupting focal complex formation and producing poorly adherent lamellipodia that retract as dorsal ruffles.

molecule to stabilize the interaction between PTPφ and paxillin. Relevant to this possibility, it has been noted recently that Pyk2-deficient macrophages display morphological changes and a migratory defect (23). Our data suggest that paxillin is a specific substrate of PTPφ and that, via its association with both PTPφ and paxillin, Pyk2 stabilizes the low-affinity enzyme-substrate interaction.

Paxillin dephosphorylation by PTPφ in dorsal ruffles appears to regulate the incorporation of paxillin into focal complexes. As we have shown here in macrophages (Fig. 7d and g) and others have shown in murine mammary gland cells (31), paxillin has been identified in three distinct subcellular locations: focal contacts, the cell periphery, and diffusely in the cytoplasm. However, using phosphospecific antipaxillin antibodies, tyrosine-phosphorylated paxillin was localized at the cell periphery and in focal contacts only (31). We could not detect PTPφ in macrophage focal complexes, nor has Pyk2 been demonstrated there, despite its association with paxillin in vivo (46). Our results indicate that the only site in which PTPφ, Pyk2, and paxillin are colocalized is the dorsal ruffles, where paxillin is tyrosine phosphorylated. We suggest that the focal complex disruption and reduced adhesion induced by increased PTPφ expression is due to a direct dephosphorylation of paxillin by PTPφ in the dorsal ruffles, with a subsequent reduction in the amount of phosphorylated paxillin available for incorporation into nascent focal complexes forming on the ventral surface of protruding lamellipodia (Fig. 11).

Physiological role of PTPφ in macrophages. In a physiological context, tissue macrophages are a phagocytic and highly motile cell type, and concentration gradients of CSF-1 exist in the microenvironment promoting macrophage chemotaxis towards the higher concentrations of CSF-1 (45). Unlike fibroblasts, macrophages do not form large, well-organized focal contacts with attached stress fibers. Instead, they maintain the membrane skeleton in a more dynamic state, with poorly organized focal complexes from which arise infrequent actin bundles. Growth factor regulation of PTPφ expression appears to play an important role in the maintenance of this dynamic

state, since PTPφ, via its dephosphorylation of paxillin, modulates the ability of lamellipodia to adhere to the ECM and form nascent focal complexes (Fig. 11). Little is known about the posttranslational regulation of PTPφ activity. However, it is conceivable that extracellular gradients of CSF-1 may produce intracellular gradients of active PTPφ and consequent differentials in paxillin dephosphorylation. Taken further, this may permit the establishment of more adherent focal complexes at the PTPφ-deficient leading edge of a cell, while higher PTPφ levels at the trailing edge would disrupt focal complexes in the uropodium, both combining to assist chemotaxis.

PTPφ function in cell types expressing other isoforms. In contrast to the short, membrane-spanning isoforms of PTPφ expressed in macrophages and B cells, the two largest PTPφ isoforms each contain an ECD with 8 FNIII repeats. The larger of these is expressed preferentially in neurons (D. Weinstein and F. J. Pixley, unpublished observations), while the smaller, also known as GLEPP1, is expressed apically on the plasma membrane of the podocyte foot processes in the glomerular filtration barrier (41). Both neurons and podocytes display highly complex membrane architecture involving branching of membrane extensions and interaction of these branches with neighboring cells. These membrane extension complexes must be robust enough to allow continuity of networking and signaling in neurons and maintenance of the glomerular filtration barrier. On the basis of the central role of PTPφ in the regulation of macrophage focal complex formation, it is tempting to speculate that PTPφ modulates the complex, three-dimensional membrane architecture of neurons and podocytes via homotypic or heterotypic intermolecular interactions of the ECD found in the larger isoforms of PTPφ.

REFERENCES

1. **Aguiar, R. C., Y. Yakushijin, S. Kharbanda, S. Tiwari, G. J. Freeman, and M. A. Shipp.** 1999. PTPROt: an alternatively spliced and developmentally regulated B-lymphoid phosphatase that promotes G0/G1 arrest. Blood **94:** 2403–2413.

2. **Allen, W. E., G. E. Jones, J. W. Pollard, and A. J. Ridley.** 1997. Rho, Rac and Cdc4 regulate actin organization and cell adhesion in macrophages. J. Cell Sci. **110:**707–720.

3. **Allen, W. E., D. Zicha, A. J. Ridley, and G. E. Jones.** 1998. A role for Cdc42 in macrophage chemotaxis. J. Cell Biol. **141:**1147–1157.

4. **Angers-Lostau, A., J.-F. Cote, A. Charest, D. Dowbenko, S. Spencer, L. A. Lasky, and M. L. Tremblay.** 1999. Protein tyrosine phosphatase-PEST regulates focal adhesion disassembly, migration and cytokinesis in fibroblasts. J. Cell Biol. **144:**1019–1031.

5. **Arregui, C. O., J. Balsamo, and J. Lilien.** 1998. Impaired integrin-mediated adhesion and signaling in fibroblasts expressing a dominant-negative mutant PTP1B. J. Cell Biol. **143:**861–873.

6. **Astier, A., S. N. Manie, H. Avraham, H. Hirai, S. F. Law, Y. Zhang, E. A. Golemis, Y. Fu, B. J. Druker, N. Haghayeghi, A. S. Freedman, and S. Avraham.** 1997. The related adhesion focal tyrosine kinase differentially phosphorylates p130^{cas} and the Cas-like protein, p105^{HEF1}. J. Biol. Chem. **272:**19719–19724.

7. **Bailly, M., L. Yan, G. M. Whitesides, J. S. Condeelis, and J. E. Segall.** 1998. Regulation of protrusion shape and adhesion to the substratum during chemotactic responses of mammalian carcinoma cells. Exp. Cell Res. **241:** 285–299.

8. **Berg, K. L., K. Carlberg, L. R. Rohrschneider, K. A. Siminovitch, and E. R. Stanley.** 1998. The major SHP-1 binding, tyrosine-phosphorylated protein in macrophages is a member of the KIR/LIR family and an SHP-1 substrate. Oncogene **17:**2535–2541.

9. **Boocock, C. A., G. E. Jones, E. R. Stanley, and J. W. Pollard.** 1989. Colony-stimulating factor-1 induces rapid behavioural responses in the mouse macrophage cell line, BAC1.2F5. J. Cell Sci. **93:**447–456.

10. **Brady-Kalnay, S. M., A. J. Flint, and N. K. Tonks.** 1993. Homophilic binding of PTPμ, a receptor-type protein tyrosine phosphatase, can mediate cell-cell aggregation. J. Cell Biol. **122:**961–972.

11. **Burridge, K., C. E. Turner, and L. H. Romer.** 1992. Tyrosine phosphorylation of paxillin and pp125^{FAK} accompanies cell adhesion to extracellular matrix: a role in cytoskeletal assembly. J. Cell Biol. **119:**893–903.

12. **Cecchini, M. G., M. G. Dominguez, S. Mocci, A. Wetterwald, R. Felix, H. Fleisch, O. Chisholm, J. W. Pollard, W. Hofstetter, and E. R. Stanley.** 1994. Role of colony stimulating factor-1 in the establishment and regulation of tissue macrophages during post-natal development of the mouse. Development **120:**1357–1372.

13. **Chan, A. Y., S. Raft, M. Bailly, J. B. Wyckoff, J. E. Segall, and J. S. Condeelis.** 1998. EGF stimulates an increase in actin nucleation and filament number at the leading edge of the lamellipod in mammary adenocarcinoma cells. J. Cell Sci. **111:**199–211.

14. **Cheng, J., K. Wu, M. O. Armanini, N. Rourke, D. Dowbenko, and L. A. Lasky.** 1997. A novel protein-tyrosine phosphatase related to the homotypically adhering κ and μ receptors. J. Biol. Chem. **272:**7264–7277.

15. **Clark, E. A., and J. S. Brugge.** 1995. Integrins and signal transduction pathways: the road taken. Science **268:**233–239.

16. **Cote, J. F., A. Charest, J. Wagner, and M. L. Tremblay.** 1998. Combination of gene targeting and substrate trapping to identify substrates of protein tyrosine phosphatases using PTP-PEST as a model. Biochemistry **37:**13128–13137.

17. **Crowley, E., and A. F. Horwitz.** 1995. Tyrosine phosphorylation and cytoskeletal tension regulate the release of fibroblast adhesions. J. Cell Biol. **131:** 525–537.

18. **Eddy, R. J., J. Han, and J. S. Condeelis.** 1997. Capping protein terminates but does not initiate chemoattractant-induced actin assembly in dictyostelium. J. Cell Biol. **139:**1243–1253.

19. **Garton, A. J., A. J. Flint, and N. K. Tonks.** 1996. Identification of p130^{cas} as a substrate for the cytosolic protein tyrosine phosphatase PTP-PEST. Mol. Cell. Biol. **16:**6408–6418.

20. **Garton, A. J., and N. K. Tonks.** 1999. Regulation of fibroblast motility by the protein tyrosine phosphatase PTP-PEST. J. Biol. Chem. **274:**3811–3818.

21. **Gu, J., M. Tamura, R. Pankov, E. H. Danen, T. Takino, K. Matsumoto, and K. M. Yamada.** 1999. Shc and FAK differentially regulate cell motility and directionality modulated by PTEN. J Cell Biol. **146:**389–403.

22. **Guan, K. L., and J. E. Dixon.** 1991. Eukaryotic proteins expressed in *Escherichia coli*: an improved thrombin cleavage and purification procedure of fusion proteins with glutathione *S*-transferase. Anal. Biochem. **192:**262–267.

23. **Guinamard, R., M. Okigaki, J. Schlessinger, and J. V. Ravetch.** 2000. Absence of marginal zone B cells in Pyk-2-deficient mice defines their role in the humoral response. Nat. Immunol. **1:**31–36.

24. **Hynes, R. O.** 1992. Integrins: versatility, modulation, and signaling in cell adhesion. Cell **69:**11–25.

25. **Lawson, M. A., and F. R. Maxfield.** 1995. Ca^{2+}- and calcineurin-dependent recycling of an integrin to the front of migrating neutrophils. Nature **377:** 75–79.

26. **Lee, P. S. W., Y. Wang, M. G. Dominguez, Y.-G. Yeung, M. A. Murphy, D. D. L. Bowtell, and E. R. Stanley.** 1999. The Cbl proto-oncogene stimulates CSF-1 receptor multiubiquitination and endocytosis, and attenuates macrophage proliferation. EMBO J. **18:**3616–3628.

27. **Liu, F., M. A. Sells, and J. Chernoff.** 1998. Protein tyrosine phosphatase 1B negatively regulates integrin signaling. Curr. Biol. **8:**173–176.

28. **Miller, A. D., D. G. Miller, J. V. Garcia, and C. M. Lynch.** 1993. Use of retroviral vectors for gene transfer and expression. Methods Enzymol **217:** 581–599.

29. **Mitchison, T. J., and L. P. Cramer.** 1996. Actin-based cell motility and cell locomotion. Cell **84:**371–379.

30. **Morgan, C., J. W. Pollard, and E. R. Stanley.** 1987. Isolation and characterization of a cloned growth factor dependent macrophage cell line, BAC1.2F5. J. Cell. Physiol. **130:**420–427.

31. **Nakamura, K., H. Yano, H. Uchida, S. Hashimoto, E. Schaefer, and H. Sabe.** 2000. Tyrosine phosphorylation of paxillin α is involved in temporospatial regulation of paxillin-containing focal adhesion formation and F-actin organization in motile cells. J. Biol. Chem. **275:**27155–27164.

32. **Petch, L. A., S. M. Bockholt, A. Bouton, J. T. Parsons, and K. Burridge.** 1995. Adhesion-induced tyrosine phosphorylation of the p130 src substrate. J. Cell Sci. **108:**1371–1379.

33. **Pixley, F. J., P. S. W Lee, M. G. Dominguez, D. B. Einstein, and E. R. Stanley.** 1995. A heteromorphic protein-tyrosine phosphatase, PTPφ, is regulated by CSF-1 in macrophages. J. Biol. Chem. **270:**27339–27347.

34. **Roach, T. I., S. E. Slater, L. S. White, X. Zhang, P. W. Majerus, E. J. Brown, and M. L. Thomas.** 1998. The protein tyrosine phosphatase SHP-1 regulates integrin-mediated adhesion of macrophages. Curr. Biol. **8:**1035–1038.

35. **Sap, J., Y.-P. Jiang, D. Friedlander, M. Grumet, and J. Schlessinger.** 1994. Receptor tyrosine phosphatase R-PTP-κ mediates homophilic binding. Mol. Cell. Biol. **14:**1–9.

36. **Schlaepfer, D. D., C. R. Hauck, and D. J. Sieg.** 1999. Signaling through focal adhesion kinase. Prog. Biophys. Mol. Biol. **71:**435–478.

37. **Schwarzbauer, J. E.** 1991. Fibronectin: from gene to protein. Curr. Biol. **3:** 786–791.

38. **Serra-Pages, C., N. L. Kedersha, L. Fazikas, Q. Medley, A. Debant, and M. Streuli.** 1995. The LAR transmembrane protein tyrosine phosphatase and a coiled-coil LAR-interacting protein co-localize at focal adhesions. EMBO J. **14:**2827–2838.

39. **Stanley, E. R.** 2000. CSF-1, p. 911–934. *In* J. J. Oppenheim and M. Feldman (ed.), Cytokine reference: a compendium of cytokines and other mediators of host defense. Academic Press, London, England.

40. **Streuli, M., N. X. Krueger, P. D. Ariniello, M. Tang, J. M. Munro, W. A. Blattler, D. A. Adler, C. M. Disteche, and H. Saito.** 1992. Expression of the receptor-linked protein tyrosine phosphatase LAR: proteolytic cleavage and shedding of the CAM-like extracellular region. EMBO J. **11:**897–907.

41. **Thomas, P. E., B. L. Wharram, M. Goyal, J. E. Wiggins, L. B. Holzman, and R. C. Wiggins.** 1994. GLEPP1, a renal glomerular epithelial cell (podocyte) membrane protein-tyrosine phosphatase. J. Biol. Chem. **269:**19953–19662.

42. **Tonks, N. K., and B. Neel.** 1996. From form to function: signaling by protein tyrosine phosphatases. Cell **87:**365–368.

43. **Tsiotra, P. C., K. Theodorakis, J. Papamatheakis, and D. Karagogeos.** 1996. The fibronectin domains of the neural adhesion molecule TAX-1 are necessary and sufficient for homophilic binding. J. Biol. Chem. **271:**29216–29222.

44. **Turner, C. E.** 1998. Molecules in focus: paxillin. Int. J. Biochem. Cell Biol. **30:**955–959.

45. **Webb, S. E., J. W. Pollard, and G. E. Jones.** 1996. Direct observation and quantification of macrophage chemoattraction to the growth factor CSF-1. J. Cell Sci. **109:**793–803.

46. **Williams, L. M., and A. J. Ridley.** 2000. Lipopolysaccharide induces actin reorganization and tyrosine phosphorylation of Pyk2 and paxillin in monocytes and macrophages. J. Immunol. **164:**2028–2036.

47. **Yeung, Y.-G., Y. Wang, D. B. Einstein, P. S. Lee, and E. R. Stanley.** 1998. Colony-stimulating factor-1 stimulates the formation of multimeric cytosolic complexes of signaling proteins and cytoskeletal components in macrophages. J. Biol. Chem. **273:**17128–17137.

48. **Yu, D. H., C.-K. Qu, O. Henegariu, X. Lu, and G.-S. Feng.** 1998. Protein-tyrosine phosphatase Shp-2 regulates cell spreading, migration, and focal adhesion. J. Biol. Chem. **273:**21125–21131.